4 December 1998

ELSEVIER

Chemical Physics Letters 297 (1998) 357–364

CHEMICAL PHYSICS LETTERS

Real-Space Analysis of Electronic Excitations in Free-Base (H_2P) and Magnesium (MgP) Porphins

Sergei Tretiak, Vladimir Chernyak, and Shaul Mukamel[1]

Department of Chemistry, University of Rochester P. O. RC Box 270216 Rochester, NY 14627-0216

Received: 12 August 1998; in final form: 21 September 1998

Abstract
The absorption spectra of Free-Base and Magnesium Porphins are analyzed using collective electronic normal modes representing the changes in charge distributions and bond-order patterns induced by the optical field. High frequency (4-6 eV) charge-transfer type excitations are identified.

I. INTRODUCTION

Photosynthesis is the process through which the Earth's biosphere harvests the sunlight energy. The primary pigments of photosynthesis are porphyrins [1]. Because of their fundamental and practical importance, these molecules have been the subject of extensive studies [2,3]. Considerable experimental and theoretical effort has been devoted to characterize the electronic structure of porphins (see Fig. 1) which are the basic building blocks of porphyrins [4–15]. The excited states of porphins has been observed using UV and photoelectron spectroscopy [6–8]. Their theoretical description was first made using the free-electron model proposed in 1949 [16,17]. The four-orbital model [18,19], and subsequent extensive Pariser-Par-Pople/CI calculations in 1965 reproduced the absorption spectra [4]. Recent semiempirical INDO/CI [5,10,11] and computationally expensive *ab initio* [12,14,15,20] methods were employed to obtain a more accurate calculation of porphin's spectra. However the nature of these optical excitations is still under debate [10,14,15,20].

The linear absorption spectra of porphins (Fig. 1 and Tables I and II) can be divided into three distinct spectral regions. The lowest Q band is weak. This transition is degenerate in MgP and is split into two lines in H_2P where the D_{4h} symmetry is broken. The higher frequency very strong Soret (B) band shows up as a sharp peak in both MgP and H_2P, whereas the following (N) transition is broad and weak. The proper assignment of these peaks in H_2P is still controversial [10,14,15]. The traditional interpretation given by Edwards [8] assigns $B_{\|}$ and $B_{\perp}$ to the two almost degenerate transitions with ~ 0.03 eV splitting at low temperature [6]. The N transition has a different nature, and it cannot be described by the 4 orbital model used for Q and B. The failure of almost all theoretical calculations to predict the weak splitting of the B transitions in H_2P and the oscillator strength of N requires a different interpretation. The weak splitting in B has been attributed to the vibrational progression in $B_{\|}$, whereas N has been assigned as $B_{\perp}$ and its electronic state which is similar to $B_{\|}$, was described by the 4 orbital model. The weak L and M high frequency transitions are rarely calculated. Theory usually overestimates their oscillator strengths (see Tables I and II).

In this paper we apply the collective electronic oscillator (CEO) approach [21,22] for calculating the absorption spectra of Free-Base (H_2P) and Magnesium (MgP) Porphins. The CEO, which is based on the TDHF approximation, makes it possible to visualize and analyze each optical transition in terms of the underlying motions of electrons and holes in real space [21,23,24]. We can then unambiguously identify which part of the molecule participates in a given optical excitation, and assess its degree of localization. We extend our analysis to the high frequency up to 6 eV region, where we trace the origin of the L and M bands.

In Section II we present the linear absorption spectra of porphins. In Section III we investigate the nature of the relevant electronic modes which dominate the linear absorption. Finally we discuss the spectroscopic trends and summarize our results in Section IV.

[1]Corresponding author. E-mail: mukamel@chem.rochester.edu

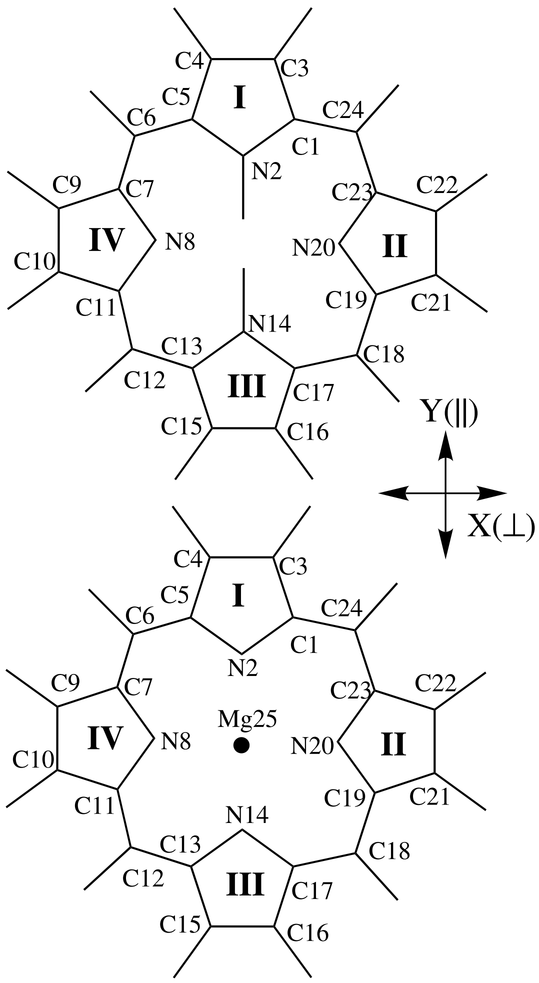

FIG. 1. Structures and atom labeling of the Free-Base Porphin (H_2P) (top) and Magnesium Porphin (MgP (bottom)

II. THE LINEAR ABSORPTION SPECTRA.

Optimal ground-state geometries of the free-base and magnesium porphins shown in Fig 1, were obtained at the 6-31G* level using Gaussian-94. MgP geometry was optimized with the Mg atom moved to $0.4\AA$ out-of-(xy)plane as suggested from the X-ray structure of chlorophyll-a [5,25]. H_2P has D_{2h} symmetry, whereas MgP possesses D_{4h} symmetry in the xy-plane. The numerical procedure has been described in detail elsewhere [22,21]. The ZINDO code was used first to generate the INDO/S hamiltonian [26–29]. We did not reparameterize this hamiltonian which has been initially fitted for the CIS level [28,29]. We next calculated the Hartree-Fock ground-state density matrices [30,31] which are the input to the following CEO calculation. The CEO/DSMA procedure [21,22] was finally applied to compute the linear absorption spectra and the relevant transition density matrices which constitutes the *electronic normal modes* ξ_ν. Each mode is a matrix representing the electronic transition between the ground state $|g\rangle$ and an electronically excited state $|\nu\rangle$. Its matrix elements are given by

$$(\xi_\nu)_{mn} = \langle \nu | c_m^+ c_n | g \rangle, \tag{2.1}$$

where $c_m^+(c_m)$ are creation (annihilation) operators of an electron at the m'th atomic orbital, and $|g\rangle$ $(|\nu\rangle)$ is the ground (excited) state many-electron wavefunction. Even though Eq. (2.1) involves matrix elements of the global many-electron eigenstates $|\nu\rangle$ and $|g\rangle$, the modes can be obtained as eigenmodes of the linearized time-dependent Hartree-Fock (TDHF) equations of motion for the density matrix driven by the external field, totally avoiding the explicit calculation of many-electron eigenstates. The eigenfrequencies Ω_ν of these equations provide the optical transition frequencies [21,22]. Transition dipoles are then calculated using the dipole moment operator $\mu_{mn} = \sum_{mn} \mu_{mn} c_m^+ c_n$

$$\mu_\nu = \mathrm{Tr}(\mu \xi_\nu), \tag{2.2}$$

and the oscillator strengths are given

TABLE I. Calculated and experimental excitation energies of the free base porphin. Energies are in eV. Oscillator strengths are given in parentheses.

Trans.	CEO	RPA^a	Exp.^{b}	CIS^a	SAC-CI^c	STEOM-CCSD^d
$Q_\parallel$	1.54 (0.025)	1.46 (0.020)	1.98 (0.01)	1.70 (0.022)	1.75 (0.0001)	1.75 (0.0007)
$Q_\perp$	1.98 (0.028)	1.97 (0.033)	2.42 (0.06)	2.06 (0.033)	2.23 (0.0006)	2.40 (0.013)
$B_\parallel$	2.966 (1.122)	2.986 (1.146)	3.33 (1.15)	3.37 (1.616)	3.56 (1.03)	3.47 (0.693)
$B_\perp$	3.011 (1.272)	3.030 (1.228)		3.52 (2.411)	3.75 (1.73)	3.62 (1.20)
$N_\parallel$	4.03 (0.441)	4.00 (0.424)	3.65 (<0.1)	4.09 (1.478)	4.24 (0.976)	4.06 (0.931)
$L1_\perp$	4.53 (0.140)	4.41 (0.115)	4.25 (∼0.1)	4.42 (0.366)	4.52 (0.350)	4.35 (0.422)
$L2_\perp$	4.95 (0.236)		4.67 (∼0.1)		5.31 (0.280)	5.00 (0.153)
$M_\parallel$	5.41 (0.323)		5.50 (∼0.1)		5.45 (0.351)	5.17 (0.272)

^{a} Reference [10]
^{b} Reference [8]
^{c} Reference [14]
^{d} Reference [15]

$$f_\nu = \frac{2}{3}\Omega_\nu \mu_\nu^2. \tag{2.3}$$

Satisfactory convergence of the linear absorption was achieved using 10-15 effective electronic modes. The CEO focuses only on the optically active transitions. All calculated electronic excitations appearing in the absorption spectra of both molecules are of $\pi - \pi^*$ type.

The calculated linear absorption spectra of free-base porphin are presented and compared with experiment [8] in Table I. The calculated linear spectrum of magnesium porphin and the experimental spectra of magnesium etioporphin (MgEtio) and magnesium tetraphenylporphin (MgTPP) [9] are given in Table II. For comparison, spectra computed with semiempirical (CIS) [10,5] and *ab initio* (SAC-CI, STEOM-CCSD) [20,14,15] methods are presented as well for both molecules. The TDHF coincides with the Random Phase Approximation (RPA) for the linear optical response of many-electron systems.[1] Zerner and co-workers applied the RPA to calculate the linear absorption of H_2P up to 4.5 eV. Our low-frequency calculated spectrum is, therefore, very close to that of given in Ref. [10] [2] (see Table I) and supports all conclusions of its authors. The calculations of MgP at RPA (or TDHF) level has not been reported yet.

The CEO underestimates the lowest (Q band) excitation energies compared with experiment and other calculations for both H_2P and MgP. However, it predicts well the Q-band experimental splitting [8] (0.44 eV versus 0.447 eV) and the oscillator strengths of $Q_\parallel$ and $Q_\perp$ transitions (0.025 and 0.028 versus 0.01 and 0.06) in H_2P. The CIS procedure reproduces these values correctly as well (0.355 eV, 0.022 and 0.033) [10] whereas *ab initio* methods failed to predict the oscillator strengths (see Table I). Both the RPA calculations [10] and our CEO results slightly underestimate the excitation energies of the Soret (B) band compare with experiment and *ab initio* calculations, however, they reproduce the correct intensities and B splitting. The electronic-oscillator analysis presented in Sec. 3 shows that $B_\parallel$ and $B_\perp$ have the same electronic nature whereas N transitions in both MgP and H_2P have the same origin, which is completely different from B. This agrees with recent *ab initio* results of Gwaltney and Bartlett [15] and contradicts the calculations of Nakatsuji *et al.* [14,20] who suggested that the N peaks in MgP and H_2P have a completely different nature. The CEO frequencies of the N, L and M bands are in fair agreement with experiment for both molecules. In addition, the predicted CEO intensities of high frequency (4-6 eV) transitions in H_2P are much better compared with *ab initio* calculations.

The spectrum of MgP shows an additional charge transfer peak TX. Its transition dipole lies along the z-axis perpendicular to the molecular plane. This transition is forbidden for planar geometry and its intensity grows fast as the Mg atom is displaced out of the molecular plane. CIS level calculations performed by Zerner and co-workers [5] show that the TX frequency is extremely sensitive to the Mg position off the molecular plane. Our calculations (not shown) support this observation.

III. COLLECTIVE ELECTRONIC EXCITATIONS.

To explore the nature of the electronic motions underlying the absorption peaks and to establish a direct real-space link between the optical response and the underlying dynamics of charges, we examined relevant electronic modes which describe collective motions of electrons and holes. The diagonal elements $(\xi_\nu)_{nn}$ represent the net charge induced on the n'th atomic orbital by an external field, whereas $(\xi_\nu)_{mn}$ $n \neq m$ is the dynamical bond-order (or electronic coherence) representing the joint amplitude of finding an electron on orbital m and a hole on orbital n [21,23,24].

[1] See, for example, Chapter 8.5 in Ref. [32]. The electronic modes are identical to the transition densities of the RPA eigenvalue equation.

[2] Our input geometry is different from that of [10]

TABLE II. Calculated excitation energies of the magnesium porphin. Experimental energies are given for Mg etioporphin (MgEtio) and Mg tetraphenylporphin (MgTTP). Energies are in eV. Oscillator strengths are given in parentheses.

Trans.	CEO	MgEtio Exp.[a]	MgTTP Exp.[a]	CIS[b]	SAC-CI[c]
Q	1.79 (0.058y)	2.14	2.07	2.02 (0.07xy)	2.01 (0.00152)
B	3.09 (1.223y)	3.18	3.04	3.63 (5.13xy)	3.63 (1.99)
TX	3.93 (0.037z)			3.93 (0.04z)	
N	4.36 (0.032y)	3.82	3.96	4.28 (0.08xy)	4.15 (0.069)
L	5.14 (0.282y)	4.7	5.16	4.97 (0.95xy)	4.75 (0.00446)
M		5.23	6.20		4.89 (0.590)

[a] Reference [9]
[b] Reference [5]
[c] Reference [20]

Because all the optically allowed transitions in the linear absorption of MgP and H_2P are of $\pi - \pi^*$ type, we focused our analysis on the π-electronic parts of the density matrices. Contour plots of the ground state density matrices are shown in Fig 2. The size of the matrices is equal to the number of carbon atoms in the molecule, labeled according to Fig. 1. The ground state density matrix $\bar{\rho}$ of H_2P (panel H_2P (ρ) in Fig. 2) is dominated by diagonal and near-diagonal elements, reflecting the bonds between nearest neighbors. The blue dots on the diagonal show that the nitrogen atoms 2, 8, 14, and 20 posses an excess electronic charge, this effect is stronger for atoms 2 and 14 which do not possess a lone electronic pair. The ground state density matrix of MgP (panel MgP (ρ)) is somewhat different since all nitrogens have the same electronic charge. The magnesium atom (upper right corner of the panel) lacks electronic density. This is usually represented as Mg^{2+} ion in the formal structures of this molecule. (For a more detailed Milliken analysis [33,34] see, for example, [5]).

We next turn to the transition density matrices (electronic modes) ξ_ν. Like $\bar{\rho}$, these are also $N \times N$ matrices, however, unlike $\bar{\rho}$, these matrices are not symmetric. The off-diagonal elements $(\xi_\nu)_{mn}$ show the amplitude of having an excess a hole at n and an electron at m. Hole and electron dynamics is thus shown along the x and y axes, respectively. Panel MgP (TX) in Fig. 2 shows the charge transfer TX mode. The figure shows that the electron is transferred from the porphin ring to the $Mg(25)$ upon excitation. This transition mostly involves the pyrrole carbon atoms (e.g. 1,3,4,5 in the ring I).

Panel H_2P $(Q_\parallel)$ in Fig. 3 displays the lowest electronic mode of free base porphin. The mode is delocalized over the entire molecule and is dominated by the off-diagonal coherences between neighboring bridge carbons 5-7,11-13,17-19,23-1. The structure of $Q_\perp$ shown in H_2P $(Q_\perp)$ is similar to $Q_\parallel$ except that the largest elements are on the diagonal at the bridge carbons. The Q mode of MgP shares the features of both $Q_\parallel$ and $Q_\perp$ and is dominated by the diagonal as well as near-diagonal elements of the bridge carbons. Note that all Q electronic modes are almost symmetric with respect to the diagonal. This reflects the absence of preferable direction of motion for holes or electrons.

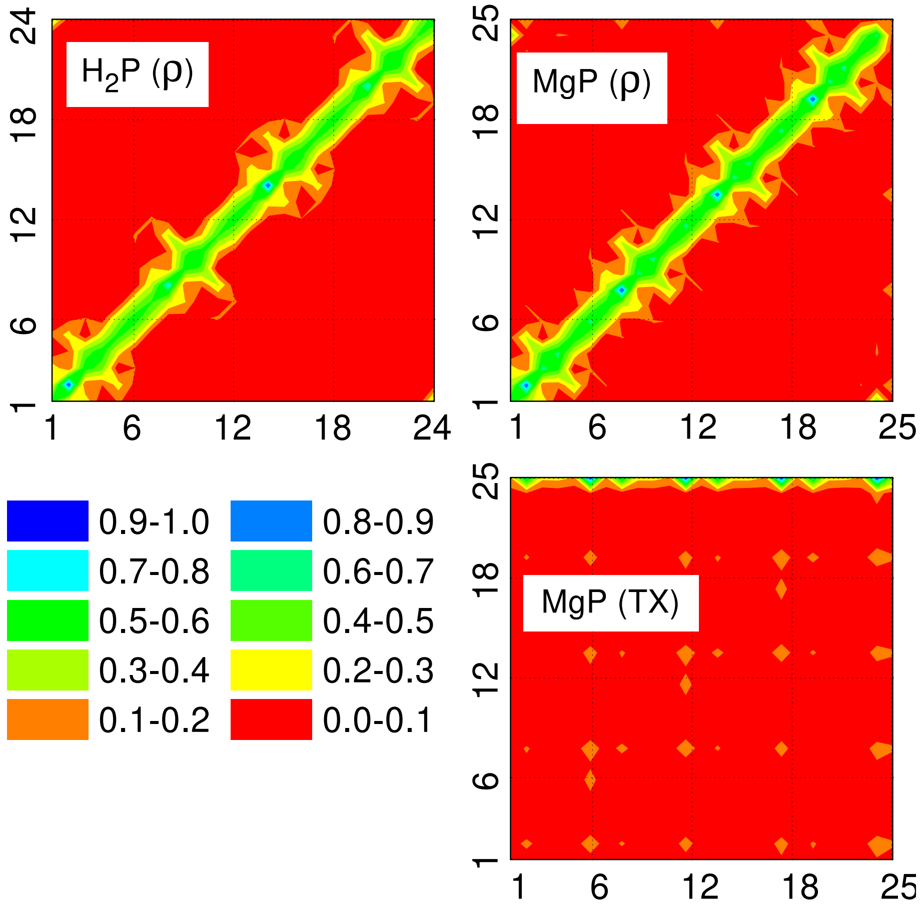

FIG. 2. Contour plots of the ground state density matrices of Free-Base Porphin (H_2P (ρ)), Magnesium Porphin (MgP (ρ)), and charge transfer electronic mode TX (panel MgP (TX)). The axes represent the carbon atoms as labeled in Fig. 1. The ordinate and abscissa label electron and hole respectively. The color code is given in the bottom left panel.

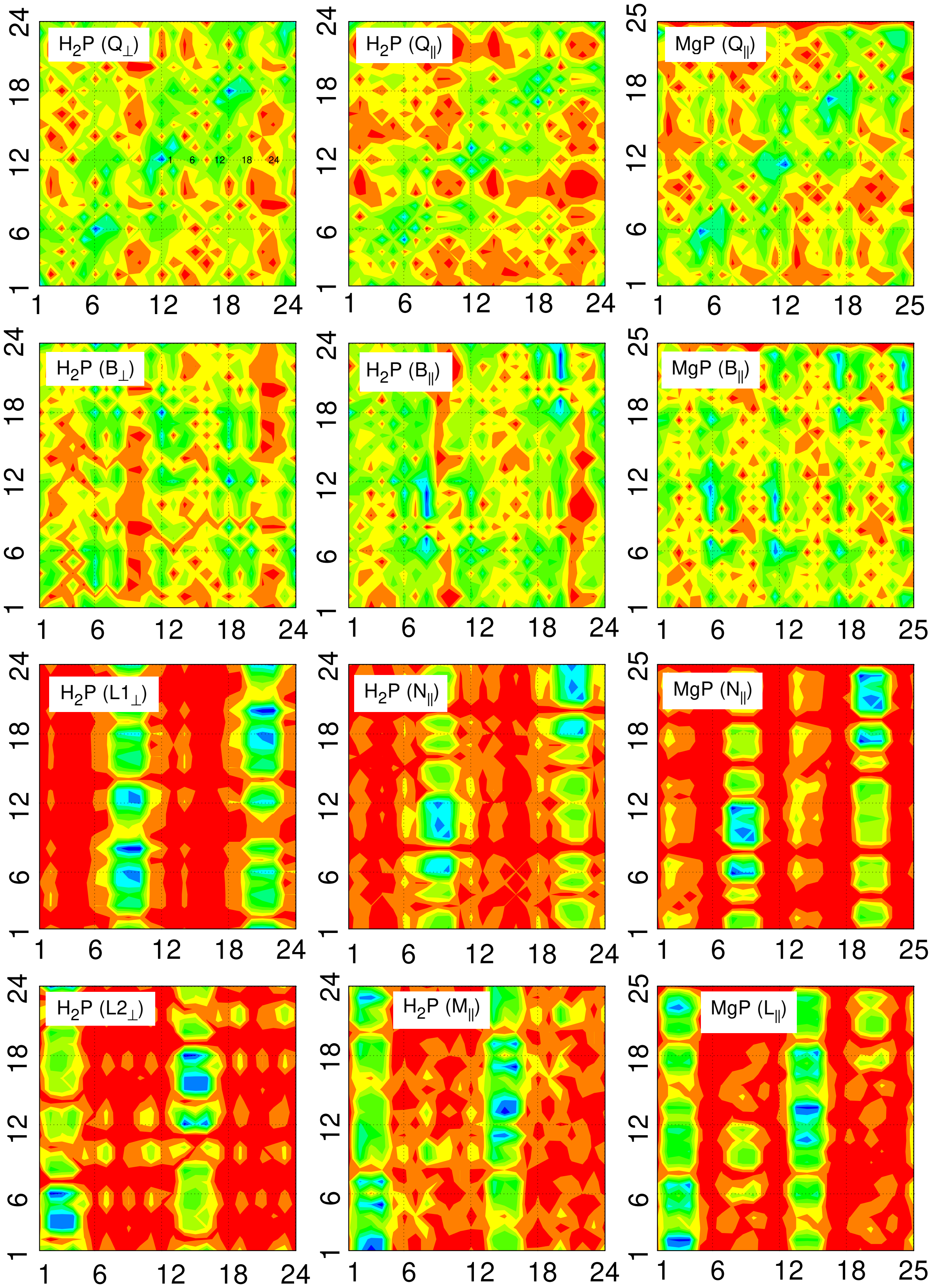

FIG. 3. Contour plots of the electronic modes which dominate the absorption spectra of Free-Base and Magnesium Porphin shown in Fig. 1. The axes represent the carbon atoms as labeled in Fig. 1. The ordinate and abscissa label electron and hole respectively. Each panel indicates the molecule (Fig. 1) and the electronic mode (Tables I and II). The color code is given in Fig. 2.

This is no longer the case for the Soret transition whose electronic modes are shown in the second row in Fig. 3. Here all modes have the same structure: they are delocalized over the entire molecule and stretched along the y (electron) direction, reflecting the charge-transfer character of the Soret band. In addition, each B-transition is dominated by a specific charge transfer process (blue elements). The preferable process in $B_\perp$ H_2P is electron transfer among bridge carbons: $6 \rightarrow 12$, $12 \rightarrow 18$, $18 \rightarrow 24$, and $24 \rightarrow 6$. $B_\parallel$ in H_2P describes electron transfer from the nitrogens to the neighboring pyrrole carbons in the II and IV rings: $8 \rightarrow 7, 9, 10, 11$ and $20 \rightarrow 19, 21, 22, 23$. $B_\parallel$ in MgP is dominated by electron transfer from the bridge carbons 6,12,18,24 to other parts of the molecule.

The N-transitions (panels H_2P $(N_\parallel)$ and MgP $(N_\parallel)$ in Fig. 3) in both H_2P and MgP are virtually the same and completely different from the low frequency transitions. The modes are localized on the two vertical "strips" and describe electron transfer from the pyrrole rings IV (left strip) and II (right strip) to the entire molecule. Despite the similarity of these electronic modes, the oscillator strength of H_2P $(N_\parallel)$ is much larger than that of MgP $(N_\parallel)$. To explain this we display in Fig. 4 the diagonal elements of these modes. It is reasonable to assume that they are primarily responsible for the transition dipole. The figure shows that the diagonal elements are the same at the pyrroles II and IV, and differ for I and III. Thus the minor diagonal delocalization of mode H_2P $(N_\parallel)$ to pyrroles I and III leads to a considerable contribution to the transition dipole. The dotted line in Fig. 4) displays the difference $\mu_n^{MgP} - \mu_n^{H_2P}$ of atomic contributions to the μ_N for these molecules. It clearly shows that the transition dipole of H_2P $(N_\parallel)$ is constructive on the I and III and destructive on the II and IV rings. Therefore, the internal hydrogens of H_2P which make rings I and III 'special' compared to MgP, provide a 12-fold increase of oscillator strength of N transition. Possible reason for the overestimated theoretical intensity of N transition in free-base porphin is that molecular vibrations restrict the delocalization of H_2P $(N_\parallel)$ to the pyrroles I and III, resulting in a dramatic reduction of the transition dipole.

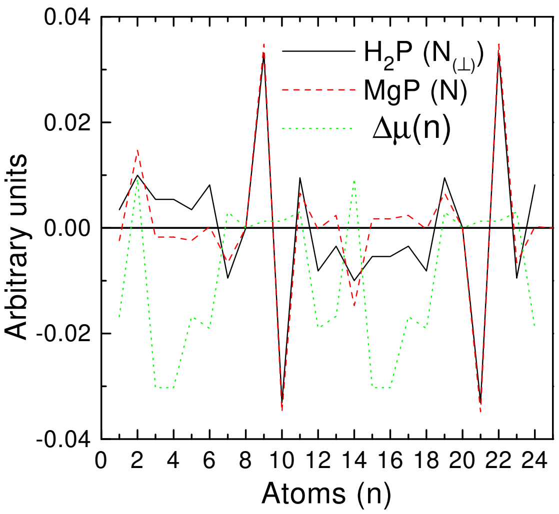

FIG. 4. Variation of the diagonal elements of modes H_2P $(N_\parallel)$ (solid line) and MgP $(N_\parallel)$ (dashed line). The X axis represents the carbon atoms as labeled in Fig. 1. The dotted line represents the difference of atomic contributions to the transition dipole of mode N in molecules H_2P and MgP: $\mu_n^{MgP} - \mu_n^{H_2P}$, $n = 1 \ldots 24$.

The higher frequency excitations in porphins have the same charge transfer character similar to the N-transition. H_2P $(L1_\perp)$ is virtually the same as H_2P $(N_\parallel)$. It has smaller delocalization to pyrroles I and III and, therefore, a weaker oscillator strength. Modes H_2P $(L2_\perp)$, H_2P $(M_\perp)$, and MgP $(L_\parallel)$ displayed at the bottom row of Fig. 3) are similar to the modes shown at the previous (third) row of this figure. However, they describe electron delocalization from pyrroles I and III to the entire molecule with a small participation of II and IV rings which provide the intensities of these transitions.

Since the modes of MgP are degenerate, we only display the $\parallel$ modes. The $\perp$ modes are obtained by simply rotating the $\parallel$ modes. For example MgP $(N_\perp)$ will describe the electron transfer from pyrroles I and III (as opposed to II and IV in MgP $(N_\parallel)$). MgP $(L_\perp)$ describes electron transfer from pyrroles II and IV (rather than I and III in $L_|$). The high frequency modes of free base porphin may be divided into pairs ($N_\parallel$, $L2_\perp$) and ($M_\parallel$, $L1_\perp$) similar to the Q and B pairs.

IV. CONCLUSIONS.

The absorption spectra of H_2P and MgP computed using the CEO method are in good agreement with experiment. Our calculations support the traditional interpretation of these spectra [8]. Coupling to vibrations is not necessary for reproducing the gross features of these spectra. The frequencies and peak intensities in the UV region up to 6 eV are accounted for as well. The computational cost is minimal - seconds[3] compared to days of extensive *ab initio* calculations [15]. In addition the real space electronic modes analysis presented in Section III reveals the nature of the corresponding optical excitations in a direct and unambiguous way. The low frequency Q bands are delocalized over the entire molecule. The intense Soret (B) transitions are also delocalized but start to show an electronic transfer character. All high-frequency excitations have specific electron transfer nature from the pyrroles to the entire molecule. They are very similar in both MgP and H_2P. However, internal hydrogens in the latter break the symmetry and finally lead to 12-fold increase of intensity of the N-band.

[3]We used a single MIPS R10000 175 MHz processor on the SGI Octane workstation.

Our real-space analysis also shows that all high-frequency transitions are degenerate in MgP and may be divided into pairs similar to the Q and B pairs in H_2P.

The CEO analysis presented in this paper does not account for Rydberg states of the molecule. They are not predicted because diffuse functions are not included in the INDO/S basis set. It has been suggested that low Rydberg states could participate in photosynthesis [7], and considerable *ab initio* effort has been devoted to address their spectroscopic signatures [12,13,15]. Most *ab initio* calculations find the lowest Rydberg state at ~ 1 eV above the Soret band. The CEO is not limited to INDO/S parameterization and could be combined with any hamiltonian which includes diffuse functions. This should allows to address Rydberg and ionized states.

ACKNOWLEDGMENTS

S. M. wishes to thank the Alexander Van Humboldt award, the Guggenhim Fellowship and the kind hospitality of Prof. Ed. Schlag at the Technical University of Munich. The support of the Air Force Office of Scientific Research (Grant No. F49620-96-1-0030), and the National Science Foundation through Grants No. CHE-9526125 and No. PHY94-15583, is gratefully acknowledged.

[1] H. Scheer, *Chlorophylls*, (CRC Press, Boca Raton Ann Arbor, Boston London, 1991).
[2] *Iron porphyrins*, edited by A. B. P. Lever, (Addison-Wesley press, Reading, MA, 1983).
[3] *Porphyrins: excited states and dynamics*, edited by M Gouterman, P. M. Rentzepis, K. D. Straub, (American Chemical Soc., Washington, D.C., 1986).
[4] C. Weiss, H. Kobayashi, and M. Gouterman, *J. Mol. Spectr.*, **16**, 415 (1965).
[5] W. D. Edwards and M. Zerner, *Int. J. of Quan. Chem.*, **23**, 1407, (1983).
[6] C. Rimington, S. F. Mason, and O. Kennard, *Spectrochim. Acta*, **12**, 65 (1958).
[7] P. Dupuis, R. Roberge, and C. Sandorfy, *Chem. Phys. Lett.*, **75**, 434 (1980).
[8] L.Edwards, D.H.Dolphin, M.Gouterman, and A.D.Adler *J.Mol.Spectroc.*, **38**, 16 (1971).
[9] L. Edwards, D. H. Dolphin, and M. Gouterman *J. Mol. Spectroc.*, **35**, 90 (1970).
[10] J. D. Baker and M. C. Zerner, *Chem. Phys. Lett.*, **175**, 192 (1990).
[11] D.C.Rawlings, E.R.Davidson, and M.Gouterman, *Theoret.Chim.Acta*, **61**, 227, (1982).
[12] D. C. Rawlings, E. R. Davidson, and M. Gouterman, *Int. J. Quantum Chem.*, **26**, 237, 251 (1984).
[13] D. C. Rawlings, M. Gouterman, E. R. Davidson, and D. Feller, *Int. J. Quantum Chem.*, **28**, 773, 797, 823 (1985).
[14] H. Nakatsuji, J. Hasegawa, and M. Hada, *J. Chem. Phys.*, **104**, 2321, (1996).
[15] S. R. Gwaltney and R. J. Bartlett, *J. Chem. Phys.*, **108**, 6790, (1998).
[16] W. T. Simpson, *J. Chem. Phys.*, **17**, 1218 (1949).
[17] H. Kuhn, *J. Chem. Phys.*, **17**, 1198 (1949).
[18] M. Gouterman, *J. Mol. Spectr.*, **6**, 138 (1961).
[19] M. Gouterman, G. H. Wagniere, and L. C. Snyder *J. Mol. Spectr.*, **11**, 108 (1963).
[20] J. Hasegawa, M. Hada, M. Nonoguchi, and H. Nakatsuji, *Chem. Phys. Lett.*, **250**, 159, (1996).
[21] S. Tretiak, V. Chernyak and S. Mukamel, *JACS*, **119**, 11408 (1997).
[22] S. Tretiak, V. Chernyak and S. Mukamel, *J. Chem. Phys.*, **105**, 8914 (1996).
[23] S. Mukamel, S. Tretiak, T. Wagersreiter, and V. Chernyak, *Science*, **277**, 781 (1997).
[24] S. Tretiak, V. Chernyak, and S. Mukamel, *J. Phys. Chem. B*, **102**, 3310-3315 (1998).
[25] C. Kratky and J. D. Dunitz, *Acta Crystallogr. B*, **31**, 1586 (1975).
[26] J. A. Pople and G. A. Segal *J. Chem. Phys.*, **43**, S136 (1965).
[27] J. A. Pople D. L. Beveridge, and P. Dobosh, *J. Chem. Phys.*, **47**, 2026 (1967).
[28] J. Ridley and M. C. Zerner, *Theor. Chim. Acta*, **32**, 111 (1973).
[29] M. C. Zerner, G. H. Loew, R. F. Kirchner, and U. T. Mueller - Westerhoff, *J. Am. Chem. Soc.*, **102**, 589 (1980).
[30] R.McWeeny and B.T.Sutcliffe, *Methods of Molecular Quantum Mechanics* (Academic Press, New York, 1976).
[31] E. R. Davidson, *Reduced Density Matrices in Quantum Chemistry* (Academic Press: New York, 1976).
[32] P.Ring and P.Schuck, *The Nuclear Many-Body Problem* (Springer-Verlag, New York, 1980).
[33] R. S. Milliken, *J.Chem.Phys.*, **23**, 1833, 1841, 2338, 2343, (1955).
[34] A. Szabo and N. S. Ostlund, *Modern Quantum Chemistry: Introduction to Advanced Electronic Structure Theory* (McGraw-Hill, New York, 1989).